ARCHITECTURAL RESEARCH, Vol. 10, No. 1(June 2008), pp. 25-32

Dynamic Instability of Lattice-Dome Structures by Lyapunov Concept

Han, Sang-Eul and Hou, Xiao-Wu
School of Architecture, Inha University, Inchon, Korea

Abstract

Stability is a very important part which we must consider in structural design. In this paper, we take advantage of finite element method to study parametrical instability of lattice dome structures, which is subjected to harmonically pulsating load. We consider elastic stiffness and geometrical stiffness simultaneously during the calculation of stiffness matrix, and adopt consistent mass matrix to make the solution more correct. In order to obtain instability regions, we represent displacements and accelerations in dynamic equation by trigonometric series expansions, and then obtain Hill's infinite determinants. After first order approximation, we can get first and second order dynamic instability regions eventually. Finally, we take 24-bar star dome and 90-bar lamella dome as examples to investigate dynamic instability phenomena.

Keywords : Dynamic Instability, Lattice-dome, Geometrical Stiffness, Instability Region

1. INTRODUCTION

Stability is a very important part we must consider in the design of large spatial structures, because lots of failures of these structures do not arise from the failure of material, but occur from the instability of structures. Therefore, it is very necessary to study their instability characteristics.

If the system is subjected to dynamic load or time dependent load, and these external loads appear in the equations of motion in the form of parameters, the system could be called parametrically excited systems. The instability relevant to these systems could be called parametrical instability.

By now, several authors have studied on parametric instability phenomena. P. Nawrotzki (1997) analyzed the stability character of shell structures according to the definition of Lyapunov instability. L. Briseghella(1998) took advantage of finite element method to study dynamic instability of beams and frames. In his paper, the key to obtain instability regions is how to solve the so called Mathieu-Hill equation. T. Most (2004) studied the dynamic instability phenomena of non-linear shell structures under random loading. The core of his method is to calculate Lyapunov exponents, and then judge stability character through these exponents. Both Partha. Dey(2006) and G. Y. Wu(2006) studied the dynamic instability of plate structures under periodic in- plane force.

All of above studies refer to the continuum, but there are little papers relevant to discrete structures. P. Nawrotzki(2000) studied dynamic instability characteristic of a two-bar truss. Thus, in this paper, we want to study dynamic instability phenomena of lattice dome structures, which can be considered as a more widely used discrete structure.

In chapter 2, we will introduce how to build stiffness matrix and mass matrix. In chapter 3, we will also introduce the definition of Lyapunov stability firstly, and then induce Hill's infinite determinants based on the equation of dynamic motion. By solving Hill's infinite determinations, we can obtain instability regions finally. In chapter 4, we investigate the instability phenomena by two examples: 24-bar star-dome and parallel lamella dome.

2. STRUCTURAL STIFFNESS MATRIX AND MASS MATRIX

2.1. STIFFNESS MATRIX

As we know, lattice dome can be considered as space truss structure, and its structural stiffness can be divided into 2 parts, elastic stiffness and geometrical stiffness. The former depends on the properties of the structure such as elastic modulus

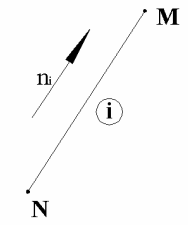

Figure 1. Typical member i

of the material E, the cross-sectional area of member A and so on. The latter depends on the external force. Apart from that, the arranging mode of the members also affects both of them. For a certain member i(as shown in Fig. 1), its elastic stiffness matrix can be formed as:

$$(K_E)_i = \begin{bmatrix} (K_E)_i^{MN} & -(K_E)_i^{MN} \\ -(K_E)_i^{MN} & (K_E)_i^{MN} \end{bmatrix} \quad (1)$$

Where, M and N are beginning point and end point of the member i.

$$(K_E)_i^{MN} = \frac{A_i \cdot E}{L_i}\begin{bmatrix} (n_i)_x^2 & (n_i)_x \cdot (n_i)_y & (n_i)_x \cdot (n_i)_z \\ (n_i)_y \cdot (n_i)_x & (n_i)_y^2 & (n_i)_y \cdot (n_i)_z \\ (n_i)_z \cdot (n_i)_x & (n_i)_z \cdot (n_i)_y & (n_i)_z^2 \end{bmatrix} \quad (2)$$

Here, $(n_i)_x$, $(n_i)_y$, $(n_i)_z$ are directional cosines of the member.

Geometrical stiffness matrix could be built as follows:

$$(K_G)_i = \begin{bmatrix} (K_G)_i^{MN} & -(K_G)_i^{MN} \\ -(K_G)_i^{MN} & (K_G)_i^{MN} \end{bmatrix} \quad (3)$$

Where,

$$(K_G)_i^{MN} = \frac{F_i}{L_i}\begin{bmatrix} 1-(n_i)_x^2 & -(n_i)_x \cdot (n_i)_y & -(n_i)_x \cdot (n_i)_z \\ -(n_i)_y \cdot (n_i)_x & 1-(n_i)_y^2 & -(n_i)_y \cdot (n_i)_z \\ -(n_i)_z \cdot (n_i)_x & -(n_i)_z \cdot (n_i)_y & 1-(n_i)_z^2 \end{bmatrix} \quad (4)$$

Where, F_i - axial force of member i

2.2. MASS MATRIX

There are two kinds of mass matrix used in FEM analysis: consistent mass matrix and lumped mass matrix.

In consistent mass matrix, the mass of element is regarded to be distributed along the element, so for a one-dimensional element, in order to build consistent mass matrix, we should assume shape functions. If the shape function is adopted as:

$$f = \begin{bmatrix} f_1 & f_2 \end{bmatrix} = \begin{bmatrix} 1-\frac{x}{L} & \frac{x}{L} \end{bmatrix} \quad (5)$$

Thus, consistent mass matrix could be obtained correspondingly.

$$M_C = \frac{\rho}{L^2}\int_0^L\int_A \begin{bmatrix} L-x \\ x \end{bmatrix} \cdot \begin{bmatrix} L-x & x \end{bmatrix} \cdot dA \cdot dx = \frac{\rho AL}{6}\begin{bmatrix} 2 & 1 \\ 1 & 2 \end{bmatrix} \quad (6)$$

While in lumped mass matrix, the mass of element is regarded to be lumped at two end points. Because of high accuracy of the former, so we use consistent mass matrix in this paper.

3. DYNAMIC INSTABILITY BY LYAPUNOV CONCEPT

As shown in Fig. 2, dynamic instability by Lyapunov concept [1],[5] is defined as follows: Suppose $x^*(t)$ is a fundamental motion of system $\dot{x} = f(x,t)$, and $x(t)$ is a neighboring motion of system. y(t)= $x(t) - x^*(t)$, which can be called as perturbation or disturbance. Fundamental motion $x^*(t)$ is called stable by Lyapunov concept if and only if, for any given ε>0, there is a corresponding $\delta(\varepsilon)$>0, such that for any initial perturbation $\|y(t_0)\| < \delta$, one has $\|y(t)\| < \varepsilon$ for all t. And if $\lim_{t\to\infty}\|y(t)\| = 0$, the fundamental motion $x^*(t)$ is called asymptotically stable.

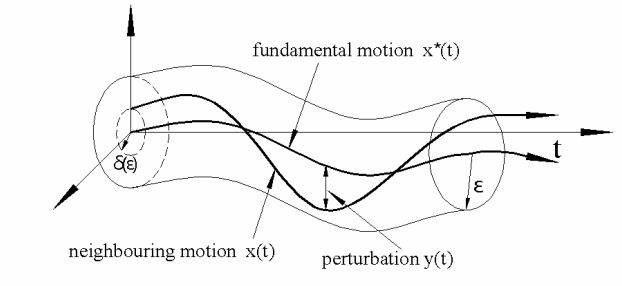

Figure 2. Dynamic stability by Lyapunov concept

For a stable motion, perturbations are insignificant, the perturbed motion stays close to the unperturbed motion. On the contrary, infinitesimal perturbation could cause a considerable change of motion in unstable case.

For nonlinear dynamic systems, Equation of motion should be represented in incremental form:

$$[M]\{\Delta \ddot{d}\} + [C]\{\Delta \dot{d}\} + [K]\{\Delta d\} = \{\Delta P\} \quad (7)$$

If time interval is adopted to be small enough, then incremental force term ΔP is also very small, so it could be ignored, this is Lyapunov's first approximation.

$$[M]\{\Delta \ddot{d}\} + [C]\{\Delta \dot{d}\} + [K]\{\Delta d\} = 0 \quad (8)$$

Here, we only consider the case of undamped system (C=0):

$$[M]\{\Delta \ddot{d}\} + [K]\{\Delta d\} = 0 \quad (9)$$

Where, $K = K_E + K_{GS} + K_{GD} \cdot \cos\Omega t$

K_E − elastic stiffness

K_{GS} − geometrical stiffness caused by time-invariant load P_S

K_{GD} − geometrical stiffness caused by time-dependent load P_D

Equation (9) is a Mathieu equation. In order to obtain the instability regions, displacement term should be represented by trigonometric series expansions:

$$\begin{cases} \Delta d = \frac{1}{2}b_0 + \sum_{k=2,4\cdots}^{\infty}(a_k \sin\frac{k\Omega t}{2} + b_k \cos\frac{k\Omega t}{2}) \; ; & \text{T} \\ \Delta d = \sum_{k=1,3\cdots}^{\infty}(a_k \sin\frac{k\Omega t}{2} + b_k \cos\frac{k\Omega t}{2}) \; ; & \text{2T} \end{cases} \tag{10}$$

And then, incremental acceleration could be obtained by differentiating above equations.

$$\begin{cases} \Delta \ddot{d} = -\frac{k^2\Omega^2}{4}\sum_{k=2,4\cdots}^{\infty}(a_k \sin\frac{k\Omega t}{2} + b_k \cos\frac{k\Omega t}{2}) \; ; & \text{T} \\ \Delta \ddot{d} = -\frac{k^2\Omega^2}{4}\sum_{k=1,3\cdots}^{\infty}(a_k \sin\frac{k\Omega t}{2} + b_k \cos\frac{k\Omega t}{2}) \; ; & \text{2T} \end{cases} \tag{11}$$

Next, we substitute these two trigonometric series into Equation (9), two systems of equations for period T and period 2T could be obtained respectively. For non-trivial solutions of a_k and b_k, Hill's infinite determinants should be zero.

Period 2T:

$$\begin{vmatrix} K_E + K_{GS} \pm 0.5K_{GD} - \frac{1}{4}M\Omega^2 & 0.5K_{GD} & 0 & \cdots \\ 0.5K_{GD} & K_E + K_{GS} - \frac{9}{4}M\Omega^2 & 0.5K_{GD} & \cdots \\ 0 & 0.5K_{GD} & K_E + K_{GS} - \frac{25}{4}M\Omega^2 & \cdots \\ \vdots & \vdots & \vdots & \vdots \end{vmatrix} = 0 \tag{12}$$

Period T:

$$\begin{vmatrix} K_E + K_{GS} - M\Omega^2 & 0.5K_{GD} & 0 & \cdots \\ 0.5K_{GD} & K_E + K_{GS} - 4M\Omega^2 & 0.5K_{GD} & \cdots \\ 0 & 0.5K_{GD} & K_E + K_{GS} - 9M\Omega^2 & \cdots \\ \vdots & \vdots & \vdots & \vdots \end{vmatrix} = 0 \tag{13}$$

$$\begin{vmatrix} K_E + K_{GS} & 0.5K_{GD} & 0 & \cdots \\ 0.5K_{GD} & K_E + K_{GS} - 4M\Omega^2 & 0.5K_{GD} & \cdots \\ 0 & 0.5K_{GD} & K_E + K_{GS} - 4M\Omega^2 & \cdots \\ \vdots & \vdots & \vdots & \vdots \end{vmatrix} = 0 \tag{14}$$

However, all above determinants are of infinite order. Here, we only consider their first-order approximation, which has been demonstrated to be a good approximation. That is to say, we only solve the following simplified eigenvalue problems. The calculation procedure is shown as fig. 3.

$$\left| K_E + K_{GS} \pm \frac{1}{2}K_{GD} - \frac{M}{4}\Omega^2 \right| = 0 \tag{15}$$

$$\left| K_E + K_{GS} - M\Omega^2 \right| = 0 \tag{16}$$

$$\begin{vmatrix} K_E + K_{GS} & K_{GD} \\ \frac{1}{2}K_{GD} & K_E + K_{GS} - M\Omega^2 \end{vmatrix} = 0 \tag{17}$$

4. NUMERICAL EXAMPLE

4.1. 24-BAR STAR DOME

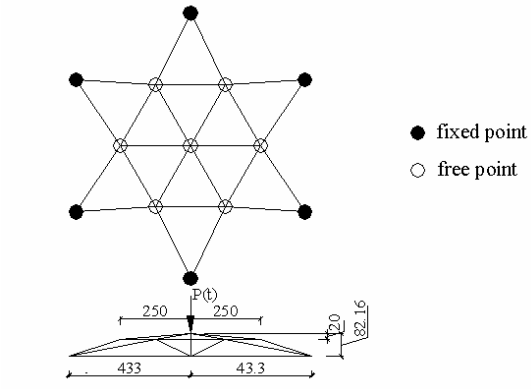

Figure 4. 24-bar star-dome (dimension: mm)

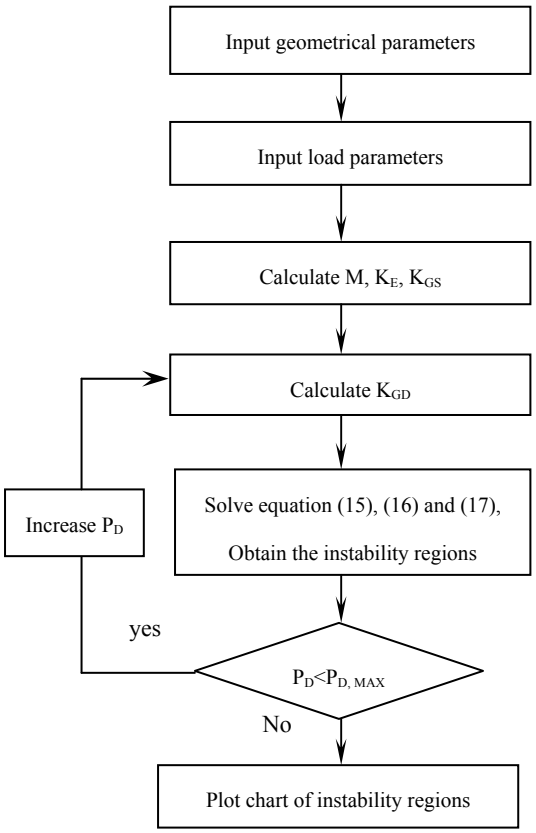

Figure 3. Flow chart for the calculation of instability regions

$$\Gamma_r = \frac{P_r}{K_r} = \frac{\{\phi_r\}^T \cdot \{F\}}{\{\phi_r\}^T \cdot \{K\} \cdot \{\phi_r\}} \tag{18}$$

According to table 1 and Fig. 5, we can know 1st mode shape and 7th mode shape play dominating roles under these two conditions. However, there are also some differences: in the first condition, the ratio of two modal participation factors $\Gamma_1 / \Gamma_7 = 30$, so we can regard that only 1st mode shape affects the response of the structure approximately. On the contrary, the ratio of two modal participation factors in the second condition $\Gamma_1 / \Gamma_7 = -1.26$, so we couldn't neglect the effect of 7th mode shape.

Table 1. Modal participation factors of major modes

Mode shape	Modal participation factor	
	Load at central point	Load at all free points
1(ω_1=41.57)	3.6*10^{-3}	2.9*10^{-3}
4(ω_4=75.71)	7.4*10^{-8}	-1.5*10^{-6}
7(ω_7=78.97)	1.2*10^{-4}	-2.3*10^{-3}
11(ω_{11}=364.94)	2.7*10^{-10}	5.1*10^{-10}
14(ω_{14}=460.11)	3.1*10^{-6}	-7.4*10^{-6}
17(ω_{17}=654.27)	8.4*10^{-12}	-3.8*10^{-11}

4.1.1. BASIC PARAMETERS

As shown in Fig. 4, the analytical model in this section is 24-bar star dome. As we know, when the star dome is loaded, it appears strong geometrical nonlinearity, and there exist bifurcation buckling phenomenon, which has been studied by lots of authors. But in this paper, we only study the dynamic instability character of this structure. It is excited by a harmonically pulsating load $P(t) = P_S + P_D \cdot \cos\Omega t$. Here, P_S term is time-invariant, and $P_D \cdot \cos\Omega t$ term is harmonically time-dependent. EA is constant for all the members with $E = 3.03 \times 10^9$ pa and $A = 3.17 \times 10^{-4} m^2$.

4.1.2. MODAL ANALYSIS OF STAR-DOME

On the base of elastic stiffness matrix and mass matrix explained in chapter 2, we can obtain the natural frequencies and mode shapes of star- dome by FEA method. And modal participation factor [11] of the r-th mode can be calculated by Equation (18). The results are shown in table 1 and Fig. 5.

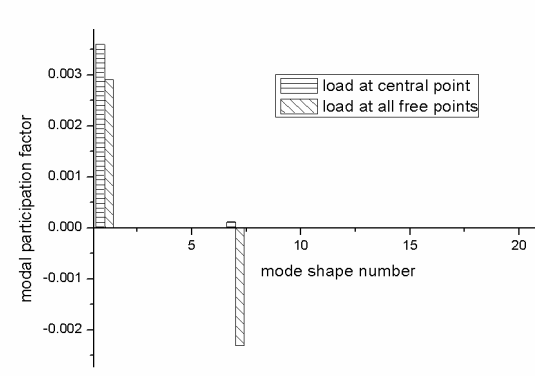

Figure. 5. Modal participation factor

4.1.3. CRITICAL LOAD OF STAR-DOME

In order to obtain the critical load, we should get the load-displacement curve of star- dome in advance. Here, the load is linearly increased. We can get the curve as shown in Fig. 6 by taking advantage of Newton-Raphson method.

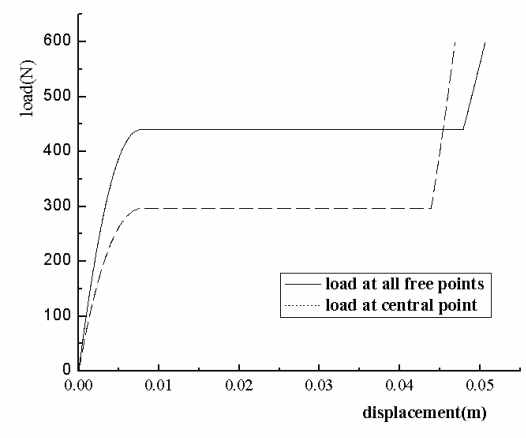

Figure 6. Load-displacement curve of Star- dome

4.1.4. INSTABILITY REGIONS

By solving above three equations (15), (16) and (17), we can obtain the first and second instability regions as shown in Fig. 7. The response curves of points in and out of the instability region are shown in Fig. 8.

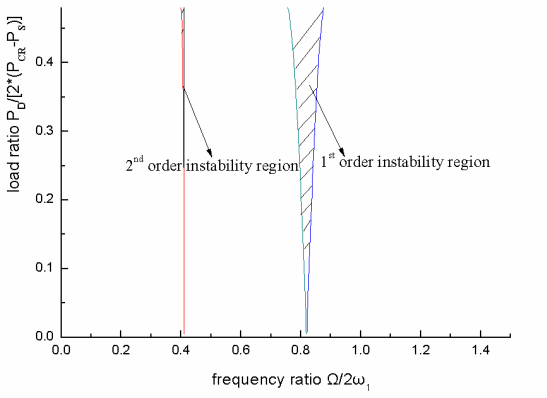

Figure 7. First and second instability regions

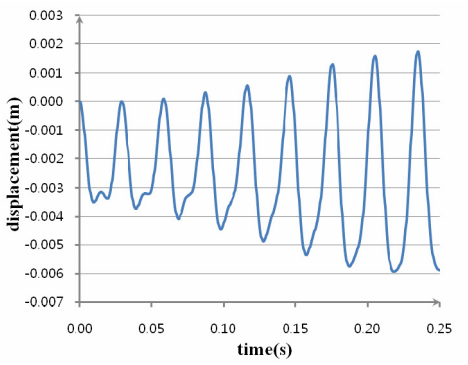

(a) Response of point in instability region

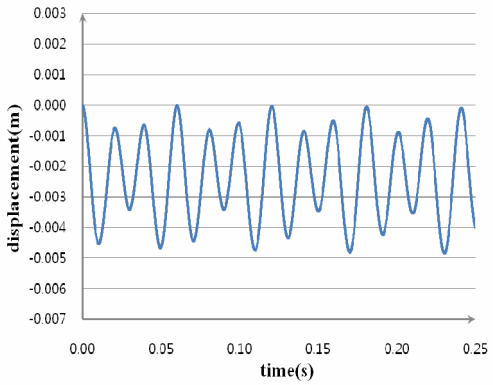

(b) Response of point in stability region

Figure 8. Dynamic response curves

In Fig.7, the data in x-axis denotes the value of external frequency, while that in y-axis denotes the value of P_D. These two values composite a point, if it is in the instability region, it means that the force with this amplitude and frequency will excite instability phenomenon.

4.2 PARALLEL LAMELLA DOME

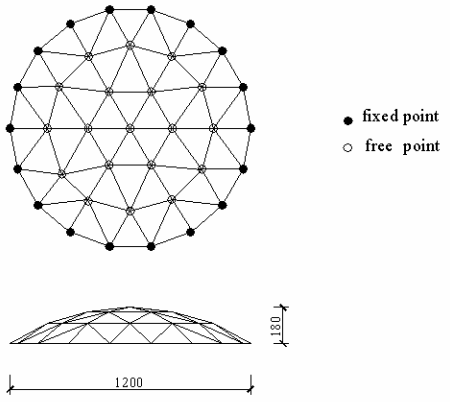

Figure 9. Parallel lamella dome (dimension: mm)

4.2.1. BASIC PARAMETERS

As shown in Fig. 9, the span of parallel lamella dome is 1.2m, and rise-span ration is 0.15. Elastic module is $E = 3.03 \times 10^9$ pa, and sectional areas of members are shown in table 2 and Fig. 10. Loading pattern is shown in Fig. 11.

Table 2. Sectional areas of members

member	*Area(m^2)*
A	$2.34*10^{-6}$
B	$3.93*10^{-6}$
C	$5.95*10^{-6}$
D	$7.07*10^{-6}$
E	$1.57*10^{-5}$
F	$2.20*10^{-5}$

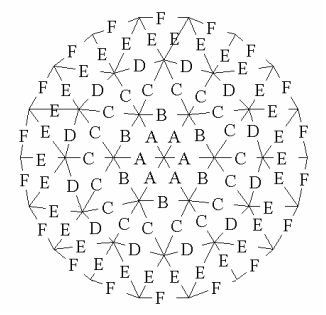

Figure 10. Distribution of Members

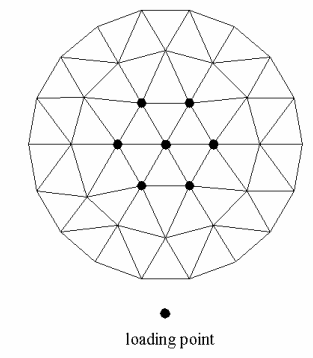

Figure 11. Loading pattern

4.2.2. MODAL ANALYSIS

Firstly, we take advantage of FEA method to calculate natural frequencies and corresponding mode shapes, and then we use the method shown in section 4.1.2 to obtain modal participation factors of each mode. Major ones of them are shown in table 3.

Different from example 4.1, where the 1st mode shape is the dominating one, but in example 4.2, the dominating mode shapes are the 8th, 9th, 18th and 19th mode shapes.

Table 3. Modal participation factors of major modes

Number of mode	*Frequency(Hz)*	*Modal Participation factor*
9	470.20	0.037
10	489.01	0.009
18	558.53	-0.006
19	721.45	0.010

4.2.3. CRITICAL LOAD P_{cr}

As narrated in the above section, we obtain load-displacement curve (as shown in Fig. 12) by taking advantage of Newton-Raphson method. From Fig. 12, we can know that the critical load is about 602N easily.

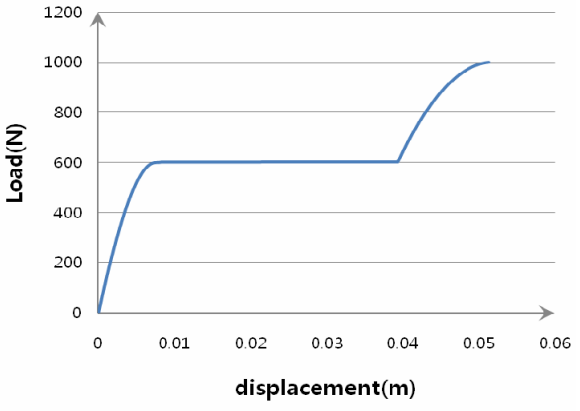

Figure 12. Load-displacement curve of lattice dome

4.2.4. INSTABILITY REGIONS

Different from example 4.1, where the 1st mode shape is the dominating one, but in example 4.2, the dominating mode shapes are the 8th, 9th, 18th and 19th mode shapes.

Here, we take the 19th mode shape as example, and analyze the instability regions of the lamella parallel dome.

By solving Equation (15), (16) and (17), we can obtain the first and second instability regions, as shown in Fig. 13. From this figure, we can know that the frequency in 1st instability region is about twice of its natural frequency, which is the same with the results of other persons' studies.

Response curves of points in and out of the instability region are shown in Fig. 14.

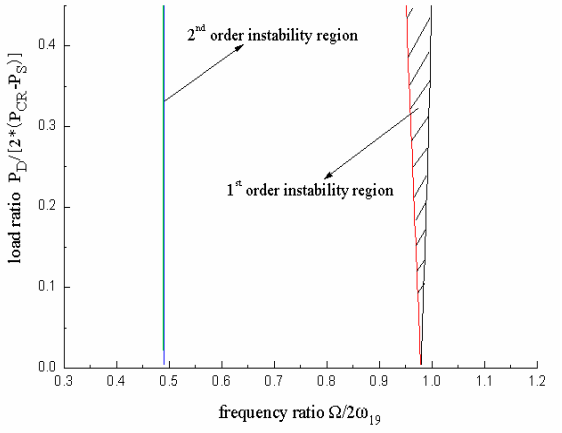

Figure 13. First and second instability regions

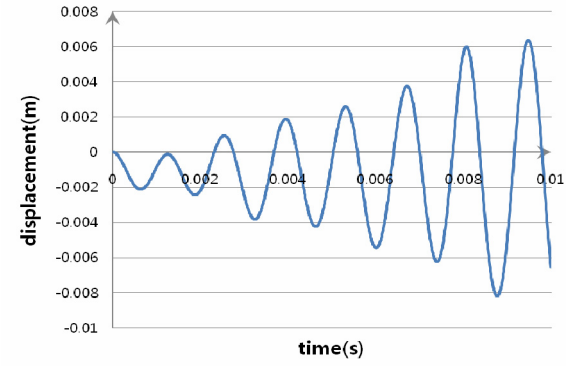

(a) Displacement of point in instability region

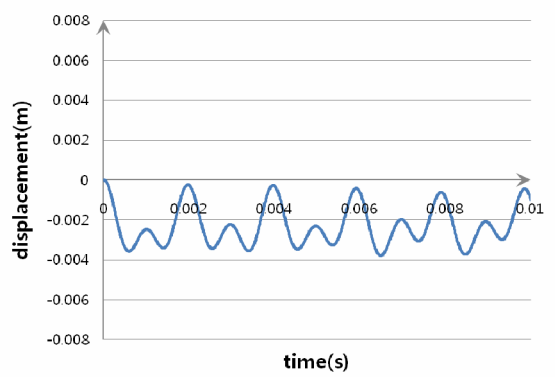

(b) Displacement of point out of instability region

Figure 14. Response curves in and out of the instability regions

5. CONCLUSION

In this paper, dynamic instability behavior of lattice dome structure under harmonically pulsating load was studied by making use of finite element method. When calculating structural stiffness, we have considered the geometrical nonlinear properties of this structure, and then we obtain the load-displacement curve and the critical load in static state by Newton-Raphson method. Finally, through solving first-order approximation of Hill's infinite determinants, we obtain dynamic instability regions.

Two numerical examples have been analyzed in this paper. For 24-bar star dome, the 1st mode shape is the dominating one. By taking advantage of the method shown in this paper, we can get its first and second instability regions. However, for parallel lamella dome, the 8th, 9th, 18th and 19th mode shapes play more important role than the 1st one. Therefore, we should calculate instability regions for these mode shapes rather than the 1st one.

In this paper, we only consider the dynamic instability phenomenon under the harmonically pulsating load. Dynamic instability phenomenon should also exist in some other conditions, such as sudden step loads and other arbitrary time-dependent loads. It will be the issue which we will study in the future.

ACKNOWLEDGEMENTS

This paper is supported by the fund of Inha University. We appreciate its help.

REFERENCES

Xie, W.C. (2006) Dynamic Stability of Structures. New York: Cambridge University Press.

Kratzig, W.B. & Niemann, H.J. (1996) Dynamics Of Civil Engineering Structures. Netherlands: A.A.Balkema

Publishers.
Levy, R. & Spillers, W.R. (1995) Analysis of Geometrically Nonlinear Structures. New York: Chapman & Hall.
Nawrotzki, P. & Eller, C. (2000) "Numerical stability analysis in structural dynamics." Computer Methods in Applied Mechanics and Engineering, 189:915-929.
Most, T., Bucher, C. & Schorling, Y. (2004) "Dynamic stability analysis of non-linear structures with geometrical imperfections under random loading." Journal of Sound and Vibration, 276:381-400.
Briseghella, L., Majorana, C.E. & Pellegrino, C. (1998) "Dynamic stability of elastic structures: a finite element approach." Computer and Structures, 69:11-25.
Nawrotzki, P., Kratzig, W.B. & Montag, U. (1997) "A Unified Computational Stability Concept for Conservative and Non-conservativ Shell Responses." Computers and Structures, 64:221-238.
Xue, Qiang. & Meek, J.L. (2001) "Dynamic response and instability of frame structures." Computer Methods in Applied Mechanics and Engineering, 190:5233-5242.
Dey, Partha. & Singha, M.K. (2006) "Dynamic stability analysis of composite skew plates subjected to periodic in-plane load." Thin-Walled Structures, 44:937-942.
Wu, G.Y. & Shih, Y.S. (2006) "Analysis of dynamic instability for arbitrarily laminated skew plates." Journal of Sound and Vibration, 292:315-340.
Tedesco, J.W., McDougal, W.G. and Ross, G.A. (1999) Structural dynamics: theory and application. California: Addison Wesley Longman.

(Data of Submission : 2008. 4. 1)